Atmos. Chem. Phys. Discuss., 14, 32935–32977, 2014
www.atmos-chem-phys-discuss.net/14/32935/2014/
doi:10.5194/acpd-14-32935-2014

Atmospheric Chemistry and Physics
Discussions
Open Access

Influence of particle phase state on the hygroscopic behavior of mixed organic–inorganic aerosols

N. Hodas[1], **A. Zuend**[2], **W. Mui**[3], **R. C. Flagan**[1,3], **and J. H. Seinfeld**[1,3]

[1]Division of Chemistry and Chemical Engineering, California Institute of Technology, 1200 E. California Blvd., Pasadena, CA, USA
[2]Department of Atmospheric and Oceanic Sciences, McGill University, Montreal, Quebec, Canada
[3]Division of Engineering and Applied Science, California Institute of Technology, Pasadena, CA, USA

Received: 20 November 2014 – Accepted: 24 November 2014 – Published: 23 December 2014

Correspondence to: N. Hodas (nhodas@caltech.edu)

Published by Copernicus Publications on behalf of the European Geosciences Union.

Abstract

Recent work has demonstrated that organic and mixed organic–inorganic particles can exhibit multiple phase states depending on their chemical composition and on ambient conditions such as relative humidity (RH). To explore the extent to which water uptake varies with particle phase behavior, hygroscopic growth factors (HGFs) of nine laboratory-generated, organic and organic–inorganic aerosol systems with physical states ranging from well-mixed liquids, to phase-separated particles, to viscous liquids or semi-solids were measured with the Differential Aerosol Sizing and Hygroscopicity Spectrometer Probe at RH values ranging from 40–90 %. Water-uptake measurements were accompanied by HGF and RH-dependent thermodynamic equilibrium calculations using the Aerosol Inorganic–Organic Mixtures Functional groups Activity Coefficients (AIOMFAC) model. In addition, AIOMFAC-predicted growth curves are compared to several simplified HGF modeling approaches: (1) representing particles as ideal, well-mixed liquids, (2) forcing a single phase, but accounting for non-ideal interactions through activity coefficient calculations, and (3) a Zdanovskii–Stokes–Robinson-like calculation in which complete separation between the inorganic and organic components is assumed at all RH values, with water-uptake treated separately in each of the individual phases. We observed variability in the characteristics of measured hygroscopic growth curves across aerosol systems with differing phase behaviors, with growth curves approaching smoother, more continuous water uptake with decreasing prevalence of liquid–liquid phase separation and increasing oxygen : carbon ratios of the organic aerosol components. We also observed indirect evidence for the dehydration-induced formation of highly viscous semi-solid phases and for kinetic limitations to the crystallization of ammonium sulfate at low RH for sucrose-containing particles. AIOMFAC-predicted growth curves are generally in good agreement with the HGF measurements. The performances of the simplified modeling approaches, however, differ for particles with differing phase states. This suggests that a single simplified modeling approach cannot be used to capture the water-uptake behavior for the diversity of particle phase behavior expected in the atmosphere. Errors in HGFs calculated with the simplified models are of sufficient magnitude to contribute substantially to error in estimates of particle optical and radiative properties, particularly for the assumption that water uptake is driven by absorptive equilibrium partitioning with ideal particle-phase mixing.

1 Introduction

Atmospheric aerosols alter the Earth's radiation budget, reduce visibility, and are associated with adverse health effects (Finlayson-Pitts and Pitts, 2000; Pöschl, 2005; Seinfeld and Pandis, 2006). The magnitude of these impacts is influenced by aerosol water content, as this is a major determinant of aerosol particle size. Further, aerosol water can impact gas-phase photochemistry and secondary organic aerosol (SOA) concentrations by serving as a sink for reactive gases and as a medium for aqueous-phase and heterogeneous reactions (Ervens et al., 2011, 2013). As a result, a clear understanding of the hygroscopicity of atmospheric aerosols is key to defining the representation of aerosol properties and behavior in atmospheric models and to improving our understanding of their impacts on climate and air quality.

Organic aerosol (OA) comprises a substantial fraction of total aerosol mass (20–90 %; Seinfeld and Pandis, 2006). Moreover, particle formation and transformation processes commonly lead to the formation of internally mixed organic–inorganic particles (Seinfeld and Pankow, 2003; Marcolli et al., 2004; Zhang et al., 2005; Murphy et al., 2006; Goldstein and Galbally, 2007; Hallquist et al., 2009). Multiple studies have sought to elucidate the hygroscopic properties of OA, as well as the influence of organic aerosol components on the hygroscopic behavior and phase transitions of inorganic salts. Much of this work has focused on single- and multi-component aerosols comprised of carboxylic, dicarboxylic, and humic acids (e.g., Prenni et al., 2001; Choi and Chan, 2002a; Brooks et al., 2004; Chan et al., 2006; Moore and Raymond, 2008; Hatch et al., 2009; Pope et al., 2010; Lei et al., 2014), as well as mixtures of organic acids

Title Page
Abstract | Introduction
Conclusions | References
Tables | Figures
◄| |►
◄ ►
Back | Close
Full Screen / Esc
Printer-friendly Version
Interactive Discussion

with inorganic salts (e.g., Cruz and Pandis, 2000; Choi and Chan, 2002b; Prenni et al., 2003; Wise et al., 2003; Brooks et al., 2004; Svenningsson et al., 2006; Sjogren et al., 2007; Gao et al., 2008). Recent studies have explored water uptake by sugars, higher molecular weight organics, and polymers (Gysel et al., 2004; Mochida and Kawamura, 2004; Tong et al., 2011; Zobrist et al., 2011; Lei et al., 2014; Xu et al., 2014). Such studies have aimed to characterize the hygroscopicity of biomass burning aerosols, highly oxygenated, aged SOA, and oligomers. This body of research has demonstrated that the water-uptake behavior of OA components and their influence on the phase transitions of inorganics depend on multiple factors, including the composition and relative amounts of the organic and inorganic aerosol fractions, the physiochemical properties of the organic components, and ambient conditions. Controlled laboratory studies have also served as a basis for the development and evaluation of thermodynamic models (Clegg et al., 2001; Chan et al., 2005; Raatikainen and Laaksonen, 2005; Clegg and Seinfeld, 2006; Marcolli and Krieger, 2006; Svenningsson et al., 2006; Moore and Raymond, 2008; Zardini et al., 2008; Zuend et al., 2011; Lei et al., 2014), with the aim of representing water uptake by organic and mixed organic–inorganic aerosols.

Current regional and global chemical transport models include a simplified treatment of aerosol hygroscopicity. In CMAQ (Community Multi-scale Air Quality model), for example, water uptake only by the inorganic fraction is considered (Binkowski and Roselle, 2003; http://www.epa.gov/AMD/Research/Air/aerosolModule.html). In WRF-Chem (Weather Research and Forecasting model coupled with Chemistry), aerosol hygroscopicity depends on the aerosol module implemented. In MADE (Modal Aerosol Dynamics model for Europe) and MOSAIC (Model for Simulating Aerosol Interactions and Chemistry), only the inorganic aerosol components are considered in estimates of aerosol liquid water (Zaveri et al., 2008). In GOCART (Goddard Chemistry Aerosol Radiation and Transport), however, the influence of water uptake on the optical properties of OA is prescribed in tabulated, RH-dependent growth factors (Koepke et al., 1997; http://acmg.seas.harvard.edu/geos). The Modal Aerosol Module (MAM) assumes the hygroscopicity of primary and secondary organic aerosol can each be described with a single parameter based on Köhler theory (κ; Petters and Kreidenweis, 2007). Similarly, aerosol water associated with organic aerosol components is considered in GEOS-Chem (Goddard Earth Observing System coupled with chemistry) using a set of RH-dependent HGFs for total particulate organic carbon (http://wiki.seas.harvard.edu/geos-chem/index.php/Aerosol_optical_properties). In the Advanced Particle Microphysics (APM) module of GEOS-Chem, hygroscopicity is again parameterized based on Köhler theory (Yu et al., 2012). When water uptake by both inorganic and organic components is taken into account in these large-scale chemical transport models, total aerosol liquid water concentrations are commonly calculated either assuming particles are externally mixed or using a volume- or mass-weighted average of the κ values or water contents of all simulated components (Drury et al., 2008; Yu et al., 2012). This simplified treatment of water uptake leads to substantial uncertainties in predicted direct and indirect radiative forcing of atmospheric aerosols (Chung and Seinfeld, 2002; Kanakidou et al., 2005; Liu and Wang, 2010). Further, the assumption of external or additive mixing of the aerosol components fails to account for the influence that particle mixing state and particle-phase morphology can have on aerosol hygroscopicity and optical properties.

Recent work has demonstrated that organic and mixed organic–inorganic particles can exist in multiple phase states depending on their chemical composition and on ambient conditions such as RH and temperature (Cappa et al., 2008; Zobrist et al., 2008; Ciobanu et al., 2009; Virtanen et al., 2010; Bertram et al., 2011; Koop et al., 2011; Krieger et al., 2012). For example, non-ideal interactions between aerosol components can result in a liquid–liquid phase separation (LLPS) in which an inorganic-electrolyte-rich phase and an organic-rich phase co-exist within a single particle (Erdakos and Pankow, 2004; Ciobanu et al., 2009; Zuend et al., 2010; Bertram et al., 2011; Song et al., 2012a; Zuend and Seinfeld, 2012; You et al., 2013, 2014). Laboratory studies have demonstrated that ambient OA can exist as a highly viscous liquid, semi-solid, or glass under atmospherically relevant conditions (Zobrist et al., 2008, 2011; Mikhailov et al., 2009; Koop et al., 2011; Tong et al., 2011). Amorphous solid (glassy) SOA has been observed both in a laboratory chamber and in the field (Virtanen et al., 2010; Saukko et al., 2012). Such complex phase behavior has major implications for the partitioning of water and semi-volatile organic species to the particle phase (Ciobanu et al., 2009; Koop et al., 2011; Krieger et al., 2012; Mikhailov et al., 2009; Bones et al., 2012; Song et al., 2012a, 2014; Zaveri et al., 2014). Diffusion coefficients in solid or semi-solid particles have been estimated to be up to seven orders of magnitude smaller than in liquids (Vaden et al., 2011; Abbatt et al., 2012), resulting in the inhibition of mass transfer through the aerosol bulk and delayed uptake and evaporation of water (Koop et al., 2011; Bones et al., 2012; Shiraiwa et al., 2011, 2013; Lienhard et al., 2014). Assuming that multi-component particles exist as well-mixed, single phase liquids when two separate phases are actually present can result in errors as large as 200 % in predicted particle mass formed through the partitioning of organic vapors to the condensed phase (Zuend et al., 2010; Zuend and Seinfeld, 2012). The present study explores the extent to which phase separations and other complex phase behavior influence the partitioning of water vapor to the particle phase.

A variety of methods have been used to characterize the factors that influence the prevalence of LLPS and amorphous solid OA. Coupling single-particle techniques with microscopy has enabled the observation of particle phase transitions with changing ambient conditions (Krieger et al., 2012). Song et al. (2012a), for example, evaluated the prevalence of LLPS as a function of RH and characterized the chemical composition of phases present within mixed organic–inorganic aerosols using a high-speed video camera and Raman microscopy. Moisture-induced glass transitions have been observed for sucrose solutions using single particle techniques and differential scanning calorimetry (Zobrist et al., 2008, 2011). Similarly, phase states (solid/semi-solid vs. liquid) of SOA as a function of RH have been inferred based on the fraction of particles that bounced when impacted on a steel substrate (Sauuko et al., 2012). A combination of bounce-fraction measurements and electron microscopy of newly formed OA in a boreal forest provided the first evidence that SOA formed in the atmosphere can behave as amorphous solids (Virtanen et al., 2010). These analyses have also shown that phase separation and particle viscosity vary with chemical composition (e.g., the organic : inorganic mass ratio), the molecular properties of the organic fraction of the aerosols (e.g., oxygen : carbon [O : C] ratio, molar mass, hydrophilicity), and RH (Bertram et al., 2011; Song et al., 2012a, b; You et al., 2013). While these studies have provided valuable information regarding the influence of RH and particle water content on particle phase state, investigations of the influence of complex phase behavior on water uptake are limited. Further, the single-particle techniques commonly used to study particle-phase morphology generally require particle sizes on the order of 1–10 µm (Krieger et al., 2012). There is a need for the study of the properties and behavior of submicrometer particles with complex phase morphologies. Herein, we explore variability in the hygroscopic behavior of accumulation-mode particles with phase morphologies ranging from well-mixed liquids, to phase-separated particles, to amorphous solids or semi-solids and evaluate the importance of accounting for such complex phase states and related phase transitions when modeling water uptake.

2 Methods

2.1 Hygroscopic growth factor measurements

Diameter hygroscopic growth factors of nine laboratory-generated aerosol systems that serve as atmospheric aerosol surrogates were measured at RHs ranging from 40 to 90 % with the Differential Aerosol Sizing and Hygroscopicity Spectrometer Probe (DASH-SP). The DASH-SP has been described in detail previously (Sorooshian et al., 2008). Briefly, in the DASH-SP, aerosols are dried in a Nafion dryer, pass through a ^{210}Po neutralizer, and are then size-selected with a differential mobility analyzer, resulting in a monodisperse aerosol population. The size-selected aerosols are split into four flows in which they are exposed to humidified air in parallel Nafion humidifiers at four controlled and different RH values. Residence times in both the Nafion dryer and the humidifiers are 4 s. The size distributions of the particles following humidification are measured with four dedicated optical particle counters (OPCs). A data processing algorithm that accounts for the dependence of the OPC signal on particle diameter and refractive index has been developed to calculate wet particle diameter (i.e., particle diameter after exposure to humidified air) from the OPC signal (Sorooshian et al., 2008). This calculation requires knowledge of the refractive index of the dry particle. One of the flow regions of the DASH-SP is kept dry (RH $< 8\,\%$) to enable calculation of the effective refractive index using an empirical relationship between OPC signal height, refractive index, and particle size. This empirical relationship was developed using calibration salts with known refractive indices (Sorooshian et al., 2008). It is assumed that the particles are spherical and scatter, but do not absorb, light. Hygroscopic diameter growth factors are calculated as the ratio of the mode diameter of the wet particle size distribution (i.e., at a 40–90 % RH set point) to the dry mode particle diameter (HGF $= D_{\text{wet}}/D_{\text{dry}}$). In this work, HGFs were measured for particles with dry mobility diameters of 250 nm. HGF measurements were performed at room temperature (~ 298 K). A minimum of 1500 particles were counted and sized at each RH value to produce the dry and wet size distributions. Experiments were repeated ten times for each aerosol system and reported growth factors were calculated as the average across those ten runs. The overall average uncertainty in DASH-SP-measured HGFs is approximately 5 %, but can approach 8 % at lower values of RH (Sorooshian et al., 2008).

With the aim of exploring the extent to which water uptake varies with particle phase state, hygroscopic growth curves were measured for chemical systems for which particle phase behavior as a function of RH has previously been characterized. For all systems studied here, RH-dependent phase states were observed at room temperature in previous work. Those studies were mainly based on single-particle techniques, in which a single-particle (typically supermicron-sized) is isolated in a controlled environment and probed with various optical and microscopy techniques. Full study details are available elsewhere (Tong et al., 2011; Zobrist et al., 2011; Song et al., 2012a; You et al., 2013). Briefly, You et al. (2013) explored the prevalence of liquid–liquid phase separations as a function of RH for internally mixed organic–inorganic aerosol systems comprising one organic compound and one inorganic salt. Single particles were deposited on a glass slide coated with a hydrophobic substrate that was then mounted in a RH- and temperature-controlled flow cell. Phase transitions during RH cycling were observed with an optical reflectance telescope. Song et al. (2012a) studied the phase behavior of more complex particle mixtures, each consisting of three dicarboxylic acids with 5, 6, or 7 carbon atoms (C_5, C_6, C_7) and ammonium sulfate, deposited on a glass slide using a Raman microscope equipped with a high-speed camera. Zobrist et al. (2011) and Tong et al. (2011) studied the phase-state and water-uptake behavior of sucrose particles using an electrodynamic balance coupled with various optical techniques and optical tweezers coupled with brightfield imaging, respectively.

A total of seven aerosol systems with RH-dependent phase morphologies ranging from well-mixed liquids, to phase-separated particles, to amorphous solids or semisolids were chosen for study in the present work from the above-described studies. Table 1 summarizes the compositions and phase behaviors of these chemical systems as determined in these prior studies. Two additional chemical systems consisting of sucrose and ammonium sulfate with varying organic : inorganic ratios were also studied here. A concurrent study (Robinson et al., 2014) also explored the hygroscopic behavior of submicron sucrose–ammonium sulfate particles, with the aim of characterizing the influence of glassy aerosol components on the optical properties of organic–inorganic particles. Sucrose was selected as a model compound in that work due to its high glass-transition temperature, as characterized by Zobrist et al. (2008). The phase states of these systems as a function of RH, however, have not been directly characterized with single-particle techniques.

In addition to differences in phase behavior, the aerosol systems represent variations in their complexity (in terms of dry composition). Particle compositions range from single-component organic systems, to two-component systems consisting of one organic and ammonium sulfate, to more complex systems consisting of dicarboxylic acid mixtures and ammonium sulfate (Table 1). To evaluate the performance of the

DASH-SP and the HGF-calculation algorithm, control runs were also performed for pure ammonium sulfate aerosols. For all chemical systems, aerosols were generated by atomizing aqueous solutions prepared by dissolving the organic and inorganic components with the mass ratios given in Table 1 in Milli-Q water (resistivity ≥ 18.2 MΩ cm). All organic components were purchased from Sigma Aldrich with purities ≥ 98 %, with the exception of the ACS reagent grade sucrose, which was purchased from Macron Fine Chemicals. Ammonium sulfate was also purchased from Macron Fine Chemicals with a purity of ≥ 99 %.

2.2 Modeling hygroscopic growth

Hygroscopic growth curves were modeled for the nine aerosol systems with the Aerosol Inorganic–Organic Mixtures Functional groups Activity Coefficients (AIOMFAC) model (Zuend et al., 2008, 2010, 2011; Appendix A). AIOMFAC is a thermodynamic model that explicitly accounts for molecular interactions between all components in an aqueous solution through the calculation of activity coefficients. A group-contribution concept based on UNIFAC (UNIversal quasi-chemical Functional group Activity Coefficients), in which the thermodynamic properties of organic compounds are determined on the basis of their molecular structures, is employed to account for interactions between organic functional groups, inorganic ions, and water (Zuend et al., 2008, 2011). In these AIOMFAC-based equilibrium calculations, the potential existence of a LLPS is determined and corresponding liquid-phase compositions are computed by the method of Zuend and Seinfeld (2013). Diameter growth factors are calculated for RH values ranging from near 0 to 99 % for both dehydration (from high RH to low RH) and hydration (low RH to high RH) cycles for all systems. For dehydration-branch calculations, growth factors at RH values lower than the particle/inorganic salt deliquescence point are representative of metastable conditions, where a supersaturated solution is present with respect to the dissolved inorganic salt. Hydration calculations include the presence of a solid inorganic phase at RH values before the full deliquescence of ammonium sulfate and the partial dissolution of ammonium sulfate into the aqueous organic solution (solid–liquid equilibrium; SLE). The hydration calculations are the most relevant to the hygroscopic growth experiments, as the atomized aerosols were dried before being exposed to elevated humidities in the DASH-SP. AIOMFAC-calculated diameter growth factors are compared to measured values to provide a detailed evaluation of the interactions likely to be occurring between aerosol chemical components.

Following Zuend and Seinfeld (2012), in addition to the full AIOMFAC-based equilibrium calculations, several simplified calculations were performed to explore the influence of phase separation and the effects of other non-ideal interactions on hygroscopic growth. These comparisons also evaluate the need for accounting for such interactions in modeling the water-uptake behavior of atmospheric aerosols. Two hygroscopic growth calculations in which no LLPS was allowed to occur were performed: (1) one in which non-ideal interactions are taken into account through AIOMFAC-calculated activity coefficients and (2) one in which it is assumed that the condensed phase behaves as an ideal mixture. Water-uptake calculations were also performed in a mode in which complete separation between an aqueous inorganic electrolyte phase and an organic phase is assumed and, thus, no organic-ion interactions are accounted for. This latter case is similar to a Zdanovskii–Stokes–Robinson (ZSR) relation assumption, since the water uptake of individual components (here two separate phases) are added up to estimate the HGF. In our ZSR-like calculation case, the influence of non-ideality on water activity, and therefore water content, is accounted for within the individual phases with AIOMFAC-based activity coefficients. A calculation in which a solid organic phase is assumed at all RH values was also performed for comparison against the DASH-SP measurements in order to evaluate whether the presence of a solid organic phase was likely in any of the chemical systems studied. All growth-curve calculations were performed at 298 K.

Note that AIOMFAC predicts phase compositions, which can be used to derive mass growth factors, but not the densities of the phases necessary to calculate diameter growth factors (assuming spherical particles). Solid and liquid-state densities of ammonium sulfate were taken from Clegg and Wexler (2011). The density of citric acid was calculated based on the data and parameterizations of Lienhard et al. (2012). The densities of all other organic compounds were estimated using the structure-based method of Girolami (1994) with the online density-calculation tools available on the E-AIM website (http://www.aim.env.uea.ac.uk/aim/aim.php). Densities of mixtures within particles and those of individual phases were calculated assuming additive molar volumes of each component (i.e., ideal mixing in terms of density).

3 Results and discussion

3.1 Experimental hygroscopic growth curves and AIOMFAC modeling

3.1.1 Two-component carboxylic acid–ammonium sulfate systems

Measured and AIOMFAC-predicted HGFs for the two-component carboxylic acid–ammonium sulfate systems (organic : inorganic dry mass ratios = 2 : 1) are shown in Fig. 1. Panels below the hygroscopic growth curves illustrate AIOMFAC predictions of the occurrence of phase separation and the composition of each phase. All of the two-component carboxylic acid–ammonium sulfate systems demonstrate suppressed water uptake at high RH values as compared to pure ammonium sulfate (Figs. 1a–c and B1). This is expected because, based on approximately linear additivity in water uptake by the different particle components, a lesser degree of water uptake by the organic fraction in comparison to inorganic salts (per unit mass) is typically the case. At RH = 80 %, ratios of the HGFs for the mixed organic–inorganic aerosols to those for pure ammonium sulfate were 0.86, 0.80, and 0.89 for the systems containing diethylmalonic acid, 2-methylglutaric acid, and citric acid, respectively. Similarly, these values were 0.87, 0.84, and 0.89 at RH = 90 %. At low to moderate RH values (40–70 %), however, the shapes and characteristics of the growth curves vary across the systems due, at least in part, to differences in phase behavior, as is discussed below.

Mixed diethylmalonic acid–ammonium sulfate particles demonstrated little to no water uptake (HGF ≈ 1.0) before the particle deliquesced at an RH of approximately 80 % (Fig. 1a). This suggest the presence of a viscous semi-solid, an amorphous solid, or a crystalline solid organic phase (with no water uptake on the timescale of the experiment). The presence of a solid organic at low to moderate RH is supported by a comparison between measured and AIOMFAC-calculated growth factors. For RH = 40–70 %, model-measurement agreement is closest for the case in which diethylmalonic acid is assumed to be solid. Measured values then approach the full equilibrium AIOMFAC calculation in which the organic is assumed to be in a liquid state. Note that all AIOMFAC-based calculations shown by the solid curves assume that the organic compounds are in a liquid-like state at all RH levels. For this system, AIOMFAC predicts a SLE state, with diethylmalonic acid dominating the liquid phase and with the solid phase fully comprised of ammonium sulfate. Following the deliquescence of ammonium sulfate at RH = 79.75 %, the particle is predicted to undergo LLPS. The organic-dominated and the ammonium sulfate-dominated phases are then predicted to merge to a single phase at RH = 94 %. The AIOMFAC-predicted RH at which merging of the two phases occurs is 5 % higher than that observed by You et al. (2013). It is likely that this small discrepancy can be attributed to uncertainty in modeled organic-ion interactions. However, it is also possible that optical methods cannot discern the presence of two phases at RH ≥ 89 % if one of the two predicted liquid phases is small in mass or volume compared to the other phase.

Like the diethylmalonic acid–ammonium sulfate system, the 2-methylglutaric-containing aerosols demonstrate a marked increase in water uptake at RH = 80 %; however, more gradual and continuous water-uptake was observed prior to particle deliquescence (Fig. 1b). Good agreement was achieved between measured and AIOMFAC-predicted growth curves at all RH values. AIOMFAC again predicts a SLE state prior to the deliquescence of ammonium sulfate at RH = 79.25 %. This is followed by the presence of two liquid phases before full merging of the phases into a single liquid phase at RH = 82.25 %. As was true for the diethylmalonic acid–ammonium sulfate system, this LLPS phase transition value is higher than the RH of 75 % observed by You et al. (2013). As noted above, this could be related to uncertainty associated with the parameterization of the AIOMFAC group-contribution method. In addition, with the gradual merging of the phases, it is possible that a remaining LLPS was not visible in the experiments at RH > 75 %.

For the citric acid–ammonium sulfate particles, measured growth factors suggest gradual, continuous water uptake at all experimental RH values (Fig. 1c). This is in agreement with measurements for this system at different dry organic : inorganic ratios reported by Zardini et al. (2008). The AIOMFAC-predicted growth curve indicates a small increase in slope with the deliquescence of ammonium sulfate at RH = 70.25 %, lower than that for pure ammonium sulfate. This is expected in the presence of a hygroscopic organic compound like citric acid (O : C = 1.17) due to the partial solubility of ammonium sulfate in the aqueous, citric acid-rich phase. Measured and predicted growth factors are in very good agreement at all RH values. For this system, a single, well-mixed liquid phase is predicted following the complete deliquescence of ammonium sulfate. This is in agreement with the experimental results of You et al. (2013), who observed no evidence of LLPS for citric acid–ammonium sulfate particles.

A comparison of hygroscopic growth curves across the three two-component systems suggests that growth curve shape reflects phase behavior in mixed organic–ammonium sulfate systems. Growth curves approach smoother, more continuous water uptake with decreasing prevalence of LLPS (i.e., looking from left to right for Fig. 1a–c). In addition to higher miscibility of the aerosol components for particles with no LLPS or those for which LLPS persists for only a small range of RH values, this can likely be attributed to the fact that both the prevalence of LLPS and aerosol hygroscopicity vary with the O : C ratios of the organic components of mixed organic–inorganic particles (Massoli et al., 2010; Bertram et al., 2011; Duplissy et al., 2011; Song et al., 2012a; You et al., 2013). Note that the O : C ratios of diethylmalonic, 2-methylglutaric, and citric acid are 0.57, 0.67, and 1.17, respectively. Thus, the smoothing of the growth curves with increasing O : C (and, incidentally, lower prevalence of LLPS) is consistent with the higher propensity of the more polar compounds to take up water and dissolve some ammonium sulfate (in a SLE) at lower RH.

3.1.2 Complex mixed dicarboxylic acid–ammonium sulfate systems

In general, water-uptake behavior was similar across the more complex dicarboxylic acid–ammonium sulfate mixtures, regardless of the carbon number of the acids included in the system and the differences in the phase morphologies of the particles observed previously in experiments by Song et al., (2012a). All systems demonstrated gradual water uptake with growth factors increasing from 1.0 to ~ 1.10 prior to a rapid increase in particle diameter of 25–34 % at RH ≈ 80 % (Fig. 2). This is in agreement with the results of Song et al. (2012a), who observed nearly complete or complete particle deliquescence at RH values of 79–80 % for all three systems. At RH ≥ 80 %, suppressed hygroscopic growth as compared to ammonium sulfate is evident, but to a lesser degree than for the two-component systems discussed above, with reductions in diameter growth factors ranging from < 1 to 11 %. This is likely attributable to the smaller organic : inorganic ratios of these systems as compared to the two-component systems (dry mass ratios of 1 : 1 rather than 2 : 1). In addition, mixing effects due to the presence of multiple organics, which can inhibit crystallization (Cruz and Pandis, 2000; Marcolli et al., 2004), likely influenced the water uptake behavior of these systems, particularly for the C_7 dicarboxylic acid–ammonium sulfate mixture. One constituent of the C_7 acid mixture, diethylmalonic acid, demonstrated behavior indicative of the presence of a crystalline solid or highly viscous organic phase in the two-component mixture discussed above. The more complex C_7 acid mixture, however, displays limited, but more gradual water uptake at low to moderate RH, suggesting a liquid (perhaps moderately viscous) phase. However, it is also possible that there was a solid–liquid phase transition around 50 % RH, where one or two of the organic compounds may have dissolved completely. If this were the case, this deliquescence behavior might be attributed to 3-methyladipic acid, as similar phase behavior has been observed for adipic acid (Zardini et al., 2008). Owing to their complexity, the multi-acid aerosol systems may provide a better analog for the majority of mixed organic–inorganic atmospheric aerosols than the two-component systems. As was true for the two-component carboxylic acid–ammonium sulfate systems, we observed a smoothing of the growth curves with increasing O:C ratio of the C_5, C_6, and C_7 dicarboxylic acid mixtures (O : C = 0.57, 0.67, and 0.8, respectively).

As determined both through previous experimental work and with the AIOMFAC modelling, there is variability in phase behavior across the mixed dicarboxylic acid–ammonium sulfate aerosol systems. For the C_5 dicarboxylic acid–ammonium sulfate system, AIOMFAC predicts a SLE state of ammonium sulfate prior to complete deliquescence at RH = 77 % (Fig. 2a). At this point, ammonium sulfate fully dissolves into the organic-dominated liquid phase. For the C_6 and C_7 systems, however, AIOMFAC predicts LLPS following the complete deliquescence of ammonium sulfate at RH = 79.25 and 79.75 %, respectively (Fig. 2b and c). For the C_6 system, the inorganic- and organic-dominated phases are then predicted to merge to a single phase at RH = 83 %, while LLPS persists up to RH = 92.75 % for the C_7 system. AIOMFAC predictions of phase behavior are in qualitative agreement with the observations of Song et al. (2012a). In agreement with AIOMFAC predictions of particle phase state during the humidification process (i.e., starting from dry conditions), no evidence of LLPS was observed for the C_5 system (Song et al., 2012a). Contrary to the experiments reported by Song et al. (2012a), AIOMFAC does predict LLPS at RH values below 80 % for the dehydration process of the C_5 system (i.e., when no solid ammonium sulfate phase is allowed to form). For both the C_6 and C_7 systems, AIOMFAC overpredicts the RH at which separated phases merge to a single phase by 10 and 3 %, respectively, in comparison to the observations by Song et al. (2012a). Song et al. (2012a) also observed differences in the morphology of the LLPS states of the C_6 and C_7 systems. For the C_6 system, an ammonium sulfate core was partially engulfed by an organic-dominated outer phase containing ammonium sulfate satellite inclusions. The C_7 system displayed a distinct, fully engulfed core-shell morphology. Despite the small degree of model-experiment disagreement in the RHs at which merging of two liquid phases occur in the C_6 and C_7 systems, good agreement between measured and AIOMFAC-predicted growth curves is achieved for the C_5, C_6, and C_7 systems (Fig. 2a–c). This suggests that the presence or absence of LLPS, as well as the morphology of LLPS (which is not taken into account in AIOMFAC), might influence water-uptake to a lesser degree than other thermodynamic properties. This is explored subsequently when we compare various modeling methods that vary in the degree to which they consider thermodynamic non-ideality and LLPS.

3.1.3 Sucrose-containing aerosols

The pure sucrose aerosols demonstrate continuous, but limited, water uptake with growth factors reaching only 1.21 at RH = 90 % (Fig. 3a). Consequently, as RH approaches 100 %, the growth factor is expected to show a steep increase. Such a steep increase is predicted by the AIOMFAC-based equilibrium model at RH ≈ 95 %. For RH ≤ 50 %, average measured values of HGF fall below the equilibrium calculations of AIOMFAC; however, this deviation is within experimental uncertainty. Previous studies demonstrated that the glass transition RH of sucrose droplets at room temperature (∼ 298 K) ranges between 25 and 53 %, depending on the rate of dehumidification (Zobrist et al., 2011; Tong et al., 2011). Thus, it is possible that a glass transition occurred with the rapid drying of the atomized sucrose droplets (residence time in Nafion dryer ∼ 4 s). However, no quantitative conclusions can be drawn about the extent to which this affected HGFs in our measurements. Nevertheless, such a glass transition may have influenced the growth factor measurement at RH < 53 % and could partially explain the observed discrepancy between the measured and modeled growth factors at those RH levels. Measured HGFs are in agreement with equilibrium-condition measurements and modeling of Tong et al. (2011) and Zobrist et al. (2011), as well as AIOMFAC-modeled HGFs, particularly at RH ≥ 60 %.

Like pure sucrose, the sucrose–ammonium sulfate systems demonstrate continuous water-uptake behavior, with smaller HGFs as compared to pure ammonium sulfate at RH = 80 and 90 % (Fig. 3b and c). The magnitude of the deviations in HGF for the sucrose–ammonium sulfate particles from those for pure ammonium sulfate varies with the organic : inorganic ratio, but is within the range observed for the other aerosol systems. At RH = 80 %, ratios of the HGFs for the sucrose–ammonium sulfate particles to those for pure ammonium sulfate were 0.87 and 0.90 for the 2 : 1 and 1 : 1 sucrose–ammonium sulfate systems, respectively. These values were 0.85 and 0.89 at RH = 90 %.

Evidence for the influence of a highly viscous phase state on hygroscopic behavior is stronger for the mixed sucrose–ammonium sulfate aerosols. While for stable thermodynamic equilibrium AIOMFAC predicts distinct deliquescence behavior at RH = 80 % for both organic : inorganic ratios, we observed smooth, continuous water uptake for RH = 40–90 % in the DASH-SP experiments (Fig. 3b and c). Note that before entering the DASH-SP, particles were dried after atomization from a solution, at which point ammonium sulfate crystallization may occur. Since the viscosity of the solution is expected to increase considerably toward lower RH, however, the high viscosity (potentially accompanied by a glass transition) may suppress the crystallization of ammonium sulfate in these systems. The corresponding AIOMFAC calculations for the humidification process are shown by the solid curves in Fig. 3 (where ammonium sulfate is in a crystalline state at low RH), while the dashed curves show the model predictions of HGF for the case where both sucrose and ammonium sulfate are present in a liquid (potentially viscous) solution. This latter scenario is often observed experimentally during a dehydration process (starting at very high RH with a homogenous liquid solution). The measured HGFs are in very good agreement with the metastable conditions of the AIOMFAC-modeled “dehydration branch.” This is in agreement with the results of Robinson et al. (2014), who also observed continuous water uptake and evidence for the inhibition of the crystallization of ammonium sulfate in the presence of viscous sucrose. Minor differences (< 10 %) in the HGFs reported in their work (RH = 60–80 %) and those described here can likely be attributed to differences in technique, as they derived growth factor based on light extinction using Mie theory, and variances in particle drying and humidification times. Our results suggest that rapid particle drying within

HGF instrumentation can induce a steep increase in particle viscosity, potentially even leading to a glass transition. As a result, such measurements may not accurately reflect the equilibrium water-uptake behavior of viscous particles. This has implications for the measurement of HGFs for ambient aerosol such as the highly oxygenated SOA for which sucrose serves as a surrogate in these experiments.

The formation of a highly viscous liquid or semi-solid phase may also lead to kinetic limitations, affecting the loss of water by evaporation during the drying process prior to humidification in the DASH-SP. There is increasing evidence from laboratory and field studies that viscous liquid or semi-solid SOA components may be present in atmospheric aerosol (e.g., Virtanen et al., 2010; Vaden et al., 2011; Saukko et al., 2012; Renbaum-Wolff et al., 2013). Thus, accounting for kinetic limitations to water uptake and release is crucial to accurately modeling the dynamic hygroscopic behavior of SOA. However, the good agreement between measured HGFs and the AIOMFAC-based dehydration-branch equilibrium calculations indicates that water loss was not substantially inhibited during particle drying. If a glassy sucrose shell had formed in these particles and this shell was of sufficient thickness to inhibit water evaporation during the 4 s residence time in the Nafion dryer, the measured effective "dry" reference diameter would have been affected by the higher water content. This oversized shell would, in turn, affect all the experimental HGFs obtained at higher RH due to the normalization by the "dry" particle diameter. If this were the case, HGFs from the experimental data would likely be lower and discrepancies from the AIOMFAC-based calculations of the dehydration growth curve would be larger. Another possible factor contributing to model-measurement disagreement for the sucrose–ammonium sulfate systems is the lower confidence in the treatment of ether groups by AIOMFAC as compared to functional groups present in the other systems studied here. This is due to limited experimental data for the development of parameterizations of ether group-ion interactions (Zuend et al., 2011). This might also contribute to uncertainty in the predicted phase behavior of the sucrose–ammonium sulfate aerosols, which indicates a SLE prior to the complete deliquescence of ammonium sulfate at RH = 80 %.

It is predicted that LLPS then persists up to RH = 94.25 % for both organic : inorganic ratios explored here (Fig. 3b and c). The predicted occurrence of LLPS for sucrose (O : C = 0.92) contrasts with previous studies that suggest that LLPS is unlikely for organic compounds with O : C > 0.7–0.8 (Bertram et al., 2011; Song et al., 2012b; You et al., 2012).

3.1.4 Measurement and modeling limitations and uncertainty

As noted above, data availability limitations and variability in experimental conditions for the datasets used in developing parameterizations of functional group-ion interactions in AIOMFAC contribute to uncertainties in ether-ion interactions and other functional-group-ion interactions. In addition, other measurement and modeling limitations can contribute to uncertainty in measured and predicted HGFs. Because experimental data regarding the densities of organic compounds are limited, the densities of many of the organic compounds studied in this work were estimated with a group-contribution method (Girolami et al., 1994). Further, for all aerosol systems and all phases present within the particles, it was assumed that the molar volumes of the aerosol components are additive (i.e., ideal mixing in terms of volume and density contributions), regardless of the thermodynamic properties of the mixture under consideration.

Complex particle-phase morphologies can also present unique sources of error and uncertainty in HGF measurement methods that use optical methods, such as the DASH-SP. For example, the algorithm that calculates diameter growth factor assumes that the refractive index of the non-water aerosol components is constant at the value measured in the dry DASH-SP channel. For systems with non-uniform surfaces (e.g., the C_6 dicarboxylic acid–ammonium sulfate system, which has been shown to have an organic outer shell with satellite ammonium sulfate inclusions or partially engulfed morphology; Song et al., 2012a), this assumption might not be accurate. In addition, the effective refractive index of the organic and inorganic particle components might evolve upon humidification as previously separated phases merge. This behavior has the potential to influence hygroscopicity measurements for systems that have core-shell morphologies at low RH to moderate RH that then transition to a single liquid-phase state with increasing water content (e.g., the C_7 dicarboxylic acid–ammonium sulfate system; Song et al., 2012a). This might contribute to non-random experimental uncertainty in the C_7 dicarboxylic acid–ammonium sulfate system. However, the overall agreement achieved between measured HGFs and AIOMFAC-calculated values in this work suggests that these factors, and their corresponding uncertainties, are not a substantial issue for the measurement of HGFs for the aerosol compositions and particle size range studied here.

In addition, as noted above, the DASH-SP HGF experiments were performed with particles much smaller than those used in the microscopy or electrodynamic balance experiments that had previously been used to directly characterize LLPS and glass transitions in the particle systems studied. Thus, the phase behavior of the particles studied here was not characterized directly. There is some limited evidence that the prevalence of LLPS can vary with particle size. Veghte et al. (2013) observed that LLPS did occur in larger particles comprised of ammonium sulfate and succinic acid or pimelic acid (diameters ≥ 170 and 270 nm, respectively), but that LLPS was not evident in smaller particles with the same composition and organic : inorganic mass ratios. While the DASH-SP experiments do not directly reveal whether a phase separation is present in the particles, the observed hygroscopic growth in comparison to the model calculations is in agreement with such phase behavior in the corresponding LLPS RH ranges.

3.2 Evaluation of simplified thermodynamic assumptions

For the multicomponent systems for which we expect that observed water-uptake behavior is governed by thermodynamic equilibrium conditions (i.e., excluding the sucrose-containing systems, which display evidence of kinetic limitations to the crystallization of ammonium sulfate), we compared the rigorous thermodynamic modeling of the AIOMFAC-based equilibrium HGF predictions to that based on several simplified thermodynamic assumptions: (1) representing particles as ideal, well-mixed liquids,

(2) forcing a single liquid phase following the deliquescence of ammonium sulfate, but accounting for non-ideal interactions through activity coefficient calculations and allowing for a SLE of ammonium sulfate, and (3) a ZSR-like calculation in which complete separation between the inorganic and organic components is assumed at all RH levels. Water is the only component allowed to partition to both phases in this ZSR-like calculation case. In all of these simplified calculation cases, the formation of a solid ammonium sulfate phase is allowed to exist (below its deliquescence point at the given temperature), except for the single-phase, ideal mixture case. We evaluate the extent to which these simple, relatively computationally inexpensive modeling approaches capture the hygroscopic behavior of particles with varied and complex phase states. Note that for the diethylmalonic acid–ammonium sulfate system, we first focus on the calculation for which the presence of a solid organic is predicted prior to particle deliquescence. At RH $\geq 80\,\%$, we then consider the full AIOMFAC equilibrium calculation in our discussion of model error, as this offered the best agreement between measured and modeled values (Fig. 1a). For all other systems, we focus on the full AIOMFAC-based equilibrium calculations at all RH values.

Figure 4 shows a comparison between the AIOMFAC-predicted HGFs for the hydration-branch of a humidity cycle and those calculated with the simplified modeling approaches. The performance of each of the simplified modeling approaches differs for particles depending on phase state. This suggests that a single simplified modeling approach cannot be used to capture the water-uptake behavior for the diversity of particle-phase behaviors expected in the atmosphere. For all systems, except the citric acid–ammonium sulfate particles, the assumption that the particles could be represented as thermodynamically ideal liquid mixtures leads to the greatest deviation from AIOMFAC-predicted growth curves. We also note that such discrepancies depend on the organic : inorganic dry state mass ratios. Generally, the smaller the ammonium sulfate mass fraction, the lower the degree of hysteresis behavior of hydration/dehydration processes. Overpredictions of diameter growth factors increase from those at low RH to a maximum just prior to the rapid increase in water uptake associated with deliquescence of ammonium sulfate, then drop to within ∼ 5 % of AIOMFAC values (Fig. 4). Maximum errors for the assumption of ideality ranged from 10–26 % and increased with increased prevalence of LLPS (i.e., looking from left to right from Fig. 4a–c and from right to left from Fig. 4d–f). For the citric acid–ammonium sulfate system, which does not undergo LLPS, ideal and AIOMFAC calculated growth curves are in good agreement for RH ≤ 80 %. Error then increases slightly to ∼ 5 %.

Not surprisingly, the forced single-phase calculations, in which non-ideal interactions are taken into account but LLPS is not, perform well for the C_5 dicarboxylic–ammonium sulfate and citric acid–ammonium sulfate systems, which demonstrated no LLPS (Fig. 4c and d). For these systems, the ZSR-like calculation leads to largest disagreement, with maximum errors of between 10 and 18 % occurring between RH values of 60 and 80 %. This can be attributed to delayed particle deliquescence in the ZSR-like calculations, since the partial dissolution of ammonium sulfate in the aqueous organic phase is not considered in this case. Similarly, for systems for which LLPS persists for only a small range of RH values, the single-phase assumption performs well, with errors never exceeding 5 % (e.g., the 2-methylgutaric–ammonium sulfate and C_6 dicarboxylic acid–ammonium sulfate systems; Fig. 4b and d). The single-phase assumption also performs well for the systems for which LLPS does occur over a wider RH range, but delayed prediction of particle deliquescence leads to a large spike in underprediction of particle diameter at RH ≈ 80 %. The good performance of the single-phase assumption at most RH values suggests that accounting for LLPS in calculations of hygroscopic growth might be less important than accounting for other non-ideal interactions between condensed-phase components. However, this result is likely not applicable to mixed organic–inorganic systems with less water-soluble (i.e., less hygroscopic) organic components, where LLPS is more prevalent and water uptake by the organic fraction is limited (Zuend and Seinfeld, 2012).

For systems that do undergo LLPS, the ZSR-like calculation also performs relatively well across the range of RH values studied, but displays discrepancies from the AIOMFAC-based equilibrium prediction of 12–18 % at moderate RH values due to deviations in the predicted SLE and deliquescence transition of ammonium sulfate. For these systems, the ZSR-like calculation also underpredicts water uptake at RH values above the point at which separated liquid phases merged to a single phase, with relative deviations approaching 10 %. As expected, growth curves begin to converge towards the AIOMFAC equilibrium predictions as RH approaches 100 % for all systems, as the solutions become very dilute (Fig. 4). Our results suggest that lack of accounting for non-ideal interactions and phase-separations leads to errors in predicted sub-saturated hygroscopic growth. Note that while maximum deviations in HGFs for the simplified approaches (compared to the AIOMFAC-based equilibrium calculation) are generally on the order of 10–25 %, the corresponding errors in particle size and refractive index can substantially impact estimates of aerosol scattering and radiative forcing (Finlayson-Pitts and Pitts, 2000).

4 Conclusions

Measurements and detailed thermodynamic modeling of the water uptake of model organic–inorganic atmospheric aerosol systems demonstrate variability in hygroscopic behavior across aerosol systems with differing RH-dependent phase behavior. Measured and modeled growth curves approach smoother, more continuous water uptake with decreasing prevalence of LLPS and increasing O : C ratios of the OA components. AIOMFAC-predicted growth curves reproduce the measured hygroscopic behavior reasonably well for all systems. A comparison between measured and modeled HGFs for the sucrose–ammonium sulfate particles indicates the presence of a viscous semi-solid phase that inhibits the crystallization of ammonium sulfate. We conclude that particle drying within HGF instrumentation may induce the formation of a highly viscous, amorphous phase (potentially accompanied by a moisture-loss-related glass transition). As a result, such measurements may not accurately reflect equilibrium water-uptake behavior. This is an important consideration when applying similar instruments to measure the hygroscopic behavior of ambient aerosols, particularly for the highly oxygenated SOA for which sucrose serves as a surrogate in our experiments. Our results add support to the growing body of literature suggesting that accounting for the influence of viscous liquid or semi-solid phases to water uptake and release can be important for accurately modeling the hygroscopic behavior of atmospheric aerosols. The performance of simplified approaches for modeling water uptake differs for particles with differing phase states/equilibria, suggesting that a single simplified modeling approach cannot be used to capture the water-uptake behavior for the diversity of particle phase behavior expected in the atmosphere. Errors in HGFs calculated using the simplified models are of sufficient magnitude to contribute substantially to uncertainties in estimates of particle optical and radiative properties. Parameterizations of LLPS and other complex phase behavior based on commonly measured variables such as O : C (e.g., Bertram et al., 2011; Koop et al., 2011; Song et al., 2012a) may prove valuable in applying the simplified HGF calculation approaches explored here in large-scale models. Finally, while the majority of field-based hygroscopicity studies focus on relatively high RH values, future measurements could also focus on the growth factors of atmospheric aerosol at low to moderate RH values, as this is the region where water-uptake behavior demonstrates the greatest variability with particle-phase behavior.

Appendix A: AIOMFAC model and phase equilibrium calculations

AIOMFAC is a group-contribution, thermodynamic model for the calculation of component activity coefficients in binary and multicomponent mixtures. It was developed to explicitly account for molecular interactions between organic functional groups and inorganic ions in aqueous solutions relevant to atmospheric aerosol chemistry. Descriptions of model details and parameterizations are available elsewhere (Zuend et al., 2008, 2010, 2011; Zuend and Seinfeld, 2012; http://www.aiomfac.caltech.edu). Herein, we provide a brief overview of the key aspects of the AIOMFAC model.

Within the model, organic molecules are represented as assemblies of functional groups. This treatment of organic molecules is based on the concept that the physiochemical properties of organic compounds can be related to their chemical structure and characteristic structural groups, which allows for treatment of the hundreds to thousands of organic compounds that characterize atmosphere organic aerosol. The organic functional groups included in AIOMFAC (alkyl (standard), alkyl (in alcohols), alkyl (in hydrophobic tails of alcohols), alkyl (bonded to hydroxyl group), alkenyl, aromatic hydrocarbons, hydroxyl, aromatic carbon-alcohol, ketone, aldehyde, ester, ether, carboxyl, hydroperoxide, peroxyacid, peroxide (organic), peroxyacyl nitrate, organonitrate) allow for the representation of a large variety of compounds observed in atmospheric aerosols. In addition AIOMFAC includes seven atmospherically-relevant cations (H^+, Li^+, Na^+, K^+, NH_4^+, Mg^{2+}, Ca^{2+}), five anions (Cl^-, Br^-, NO_3^-, HSO_4^-, SO_4^{2-}), and water.

Non-ideality (i.e., deviations from Raoult's law) in organic–inorganic aqueous solutions is accounted for through the calculation of activity coefficients for all components in a given mixture. When considering the partitioning of water vapor to a multicomponent liquid mixture, the vapor pressure of water (p_w) over the mixture is related to water activity by:

$$p_\mathrm{w} = p_\mathrm{w}^\mathrm{o} a_\mathrm{w}^{(x)} \tag{A1}$$

where $p_\mathrm{w}^\mathrm{o} = p_\mathrm{w}^\mathrm{o}(T)$ is the saturation vapor pressure over pure liquid water at temperature T and $a_\mathrm{w}^{(x)}$ is the water activity defined on a mole fraction basis. Under thermodynamic equilibrium conditions, relative humidity and water activity are related by

$$\mathrm{RH} = a_\mathrm{w}^{(x)} = \gamma_\mathrm{w}^{(x)} x_\mathrm{w} \tag{A2}$$

where $\gamma_\mathrm{w}^{(x)}$ is the activity coefficient of water on a mole fraction basis and x_w is the mole fraction of water in the particle-phase liquid mixture (here, for the case of a single liquid phase). Similarly, activity coefficients are key to accurately describing the partitioning of semi-volatile organic compounds between the gas and particle phases under thermodynamic equilibrium.

Title Page
Abstract Introduction
Conclusions References
Tables Figures
◀| |▶
◀ ▶
Back Close
Full Screen / Esc
Printer-friendly Version
Interactive Discussion

In AIOMFAC, activity coefficients are derived from expressions for the long-range, middle-range, and short-range molecular interactions that contribute to total Gibbs excess energy, which is a descriptor of the overall non-ideality of a thermodynamic system. In addition to their application in calculations of the gas-particle partitioning of water and other semi-volatile species (i.e., vapor–liquid equilibria), activity coefficients of all components in a multi-component mixture are required for the calculation of solid–liquid (SLE) and liquid–liquid equilibria (LLE). The prevalence of liquid–liquid phase separation and the composition of each phase is calculated in this work by application of AIOMFAC to compute activity coefficients in distinct liquid phases based on a reliable and efficient algorithm for finding the phase compositions that correspond to an equilibrium state. A liquid–liquid equilibrium state of a closed thermodynamic system is a state of minimum Gibbs energy of that system. The same applies to SLE and, likewise, to coupled vapor–liquid–liquid–solid equilibrium calculations, such as those performed in this work at given temperature and relative humidity to determine the number and composition of the particle phases at equilibrium. Hence, while the AIOMFAC model is at the heart of such equilibrium calculations, the distinct phases and their compositions are determined using a more general thermodynamic equilibrium model, as described by Zuend et al. (2010) and Zuend and Seinfeld (2012). For the calculation of a potential liquid–liquid phase separation, the equilibrium model essentially solves a system of nonlinear equations numerically to determine the phase state (i.e., one liquid phase vs. two liquid phases) that achieves a minimum in Gibbs energy for a given overall particle-phase composition at constant temperature and pressure. Full details regarding the algorithm used to diagnose the prevalence of LLPS and to calculate the corresponding phase composition is available in Zuend and Seinfeld (2013).

Appendix B: Control hygroscopic growth experiments

Following the same methods as described in the main text of the paper, control hygroscopic growth experiments were conducted for pure ammonium sulfate aerosols with dry mobility diameters of 250 nm. HGF experiments were conducted at room temperature (~ 298 K). The control experiments were conducted for comparison against the mixed organic–ammonium sulfate aerosol systems (i.e., to explore the influence of the organic species on the mixed organic–inorganic particle hygroscopicity when starting with the same dry size) and to evaluate the performance of the DASH-SP and the growth-factor-calculation algorithm using this well-characterized aerosol system. DASH-SP measurements reproduced previous experimental characterizations of ammonium sulfate aerosol hygroscopicity (e.g., Tang, 1980; Sorooshian et al., 2008) and are in agreement with AIOMFAC-predicted diameter growth factors (Fig. B1).

Author contributions. N. Hodas, J. H. Seinfeld, and R. C. Flagan designed the experiments. N. Hodas carried out the experiments with assistance from W. Mui. A. Zuend developed the modeling tools and performed all simulations. N. Hodas prepared the manuscript with contributions from all co-authors.

Acknowledgements. This work was supported by the National Science Foundation under Award No. 1433246 and the Office for Naval Research under Award No. N00014-14-1-0097. W. Mui was supported by an NSF Graduate Research Fellowship (Grant No. DGE-1144469) and NSF Grant No. CBET-1236909. A. Zuend was supported by a McGill University Start-up grant.

References

Abbatt, J. P. D., Lee, A. K. Y., and Thornton, J. A.: Quantifying trace gas uptake to tropospheric aerosol: recent advances and remaining challenges, Chem. Soc. Rev., 41, 6555–6581, 2012.

Bertram, A. K., Martin, S. T., Hanna, S. J., Smith, M. L., Bodsworth, A., Chen, Q., Kuwata, M., Liu, A., You, Y., and Zorn, S. R.: Predicting the relative humidities of liquid-liquid phase separation, efflorescence, and deliquescence of mixed particles of ammonium sulfate, organic material, and water using the organic-to-sulfate mass ratio of the particle and the oxygen-to-carbon elemental ratio of the organic component, Atmos. Chem. Phys., 11, 10995–11006, doi:10.5194/acp-11-10995-2011, 2011.

Binkowski, F. S. and Roselle, S. J.: Models-3 Community Multiscale Air Quality (CMAQ) model aerosol component 1. Model description, J. Geophys. Res., 108, 4183, doi:10.1029/2001JD001409, 2003.

Bones, D. L., Reid, J. P., Lienhard, D. M., and Krieger, U. K.: Comparing the mechanism of water condensation and evaporation in glassy aerosol, P. Natl. Acad. Sci. USA, 109, 11613–11618, 2012.

Brooks, S. D., DeMott, P. J., and Kreidenweis, S. M.: Water uptake by particles containing humic materials and mixtures of humic materials with ammonium sulfate, Atmos. Environ., 38, 1859–1868, 2004.

Cappa, C. D., Lovejoy, E. R., and Ravishankara, A. R.: Evidence for liquid-like and nonideal behavior of a mixture of organic aerosol components, P. Natl. Acad. Sci. USA, 105, 18687–18691, 2008.

Chan, M. N., Choi, M. Y., Ng, N. L., and Chan, C. K.: Hygroscopicity of water-soluble organic compounds in atmospheric aerosols: amino acids and biomass burning derived organic species, Environ. Sci. Technol., 39, 1555–1562, 2005.

Chan, M. N., Lee, A. K. Y., and Chan, C. K.: Responses of ammonium sulfate particles coated with glutaric acid to cyclic changes in relative humidity: hygroscopicity and Raman characterization, Environ. Sci. Technol., 40, 6983–6989, 2006.

Choi, M. Y. and Chan, C. K.: Continuous measurements of the water activities of aqueous droplets of water-soluble organic compounds, J. Phys. Chem. A, 106, 4566–4572, 2002a.

Choi, M. Y. and Chan, C. K.: The effects of organic species on the hygroscopic behaviors of inorganic aerosols, Environ. Sci. Technol., 36, 2422–2428, 2002b.

Chung, S. H. and Seinfeld, J. J.: Global distribution and climate forcing of carbonaceous aerosols, J. Geophys. Res., 107, 4407, doi:10.1029/2001JD001397, 2002.

Ciobanu, V. G., Marcolli, C., Krieger, U. K., Weers, U., and Peter, T.: Liquid–liquid phase separation in mixed organic/inorganic aerosol particles, J. Phys. Chem., 113, 10966–10978, 2009.

Clegg, S. L. and Seinfeld, J. H.: Thermodynamic models of aqueous solutions containing inorganic electrolytes and dicarboxylic acids at 298.25 K. 1. The acids as nondissociating components, J. Phys. Chem. A, 110, 5692–5717, 2006.

Clegg, S. L. and Wexler, A. S.: Densities and apparent molar volumes of atmospherically important electrolyte solutions. 1. The solutes H_2SO_4, HNO_3, HCl, Na_2SO_4, $NaNO_3$, NaCl, $(NH_4)_2SO_4$, NH_4NO_3, and NH_4Cl from 0 to 50 °C, including extrapolations to very low temperature and to the pure liquid state, and $NaHSO_4$, NaOH, and NH_3 at 25 °C, J. Phys. Chem. A, 115, 3393–3460, 2011.

Clegg, S. L., Seinfeld, J. H., and Brimblecombe, P.: Thermodynamic modeling of aqueous aerosols containing electrolytes and dissolved organic compounds, J. Aerosol Sci., 32, 713–738, 2001.

Cruz, C. and Pandis, S. N.: Deliquescence and hygroscopic growth of mixed inorganic–organic atmospheric aerosol, Environ. Sci. Technol., 32, 4313–4319, 2000.

Drury, E., Jacob, D. J., Wang, J., Spurr, R. J. D., and Chance, K.: Improved algorithm for MODIS satellite retrievals for aerosol optical depth over western North America, J. Geophys. Res., 113, D16204, doi:10.1029/2007JD009573, 2008.

Duplissy, J., DeCarlo, P. F., Dommen, J., Alfarra, M. R., Metzger, A., Barmpadimos, I., Prevot, A. S. H., Weingartner, E., Tritscher, T., Gysel, M., Aiken, A. C., Jimenez, J. L., Canagaratna, M. R., Worsnop, D. R., Collins, D. R., Tomlinson, J., and Baltensperger, U.: Relating hygroscopicity and composition of organic aerosol particulate matter, Atmos. Chem. Phys., 11, 1155–1165, doi:10.5194/acp-11-1155-2011, 2011.

Erdakos, G. B. and Pankow, J. F.: Gas/particle partitioning of neutral and ionizing compounds to single- and multi-phase aerosol particles. 2. Phase separation in liquid particulate matter containing both polar and low-polarity organic compounds, Atmos. Environ., 38, 1005–1013, 2004.

Ervens, B., Turpin, B. J., and Weber, R. J.: Secondary organic aerosol formation in cloud droplets and aqueous particles (aqSOA): a review of laboratory, field, and model studies, Atmos. Chem. Phys., 11, 11069–11102, 2011, http://www.atmos-chem-phys.net/11/11069/2011/.

Ervens, B., Wang, Y., Eagar, J., Leaitch, W. R., Macdonald, A. M., Valsaraj, K. T., and Herckes, P.: Dissolved organic carbon (DOC) and select aldehydes in cloud and fog water: the role of the aqueous phase in impacting trace gas budgets, Atmos. Chem. Phys., 13, 5117–5135, 2013, http://www.atmos-chem-phys.net/13/5117/2013/.

Finlayson-Pitts, B. J. and Pitts Jr., J. N.: Chemistry of the Upper and Lower Atmosphere, Academic Press, San Diego, CA, 2000.

Gao, Y., Yu, L. E., and Chen, S. B.: Effects of organics on the efflorescence relative humidity of ammonium sulfate or sodium chloride particles, Atmos. Environ., 42, 4433–4445, 2008.

Girolami, G. S.: A simple “back of the envelope” method for estimating the densities and molecular volumes of liquids and solids, J. Chem. Educ., 71, 962–964, 1994.

Goldstein, A. H. and Galbally, I. E.: Known and unexplored organic constituents in the Earth’s atmosphere, Environ. Sci. Technol., 41, 1514–1521, 2007.

Gysel, M., Weingartner, E., Nyeki, S., Paulsen, D., Baltensperger, U., Galambos, I., and Kiss, G.: Hygroscopic properties of water-soluble matter and humic-like organics in atmospheric fine aerosol, Atmos. Chem. Phys., 4, 35–50, doi:10.5194/acp-4-35-2004, 2004.

Hallquist, M., Wenger, J. C., Baltensperger, U., Rudich, Y., Simpson, D., Claeys, M., Dommen, J., Donahue, N. M., George, C., Goldstein, A. H., Hamilton, J. F., Herrmann, H., Hoffmann, T., Iinuma, Y., Jang, M., Jenkin, M. E., Jimenez, J. L., Kiendler-Scharr, A., Maenhaut, W., McFiggans, G., Mentel, Th. F., Monod, A., Prévôt, A. S. H., Seinfeld, J. H., Surratt, J. D., Szmigielski, R., and Wildt, J.: The formation, properties and impact of secondary organic aerosol: current and emerging issues, Atmos. Chem. Phys., 9, 5155–5236, doi:10.5194/acp-9-5155-2009, 2009.

Hatch, C. D., Gierlus, K. M, Zahardis, J., Schuttlefield, J., and Grassian, V. H.: Water uptake of humic and fulvic acid: measurements and modelling using single parameter Köhler theory, Environ. Chem., 6, 380–388, 2009.

Kanakidou, M., Seinfeld, J. H., Pandis, S. N., Barnes, I., Dentener, F. J., Facchini, M. C., Van Dingenen, R., Ervens, B., Nenes, A., Nielsen, C. J., Swietlicki, E., Putaud, J. P., Balkanski, Y., Fuzzi, S., Horth, J., Moortgat, G. K., Winterhalter, R., Myhre, C. E. L., Tsigaridis, K., Vignati, E., Stephanou, E. G., and Wilson, J.: Organic aerosol and global climate modelling: a review, Atmos. Chem. Phys., 5, 1053–1123, doi:10.5194/acp-5-1053-2005, 2005.

Koepke, P., Hess, M., Schult, I., and Shettle, E. P.: Global Aerosol Data Set, Rep. No. 243, Max-Planck-Institut für Meteorologie, Hamburg, Germany, 1997.

Koop, T., Bookhold, J., Shiraiwa, M., and Pöschl, U.: Glass transition and phase state of organic compounds: dependency on molecular properties and implications for secondary organic aerosols in the atmosphere, Phys. Chem. Chem. Phys., 13, 1923–19255, 2011.

Krieger, U., Marcolli, C., and Reid, J. P.: Exploring the complexity of aerosol particle properties and processes using single particle techniques, Chem. Soc. Rev., 41, 6631–6662, 2012.

Lei, T., Zuend, A., Wang, W. G., Zhang, Y. H., and Ge, M. F.: Hygroscopicity of organic compounds from biomass burning and their influence on the water uptake of mixed organic ammonium sulfate aerosols, Atmos. Chem. Phys., 14, 11165–11183, doi:10.5194/acp-14-11165-2014, 2014.

Lienhard, D. M., Bones, D. L., Zuend, A., Krieger, U. K., Reid, J. P., and Peter, T.: Measurements of thermodynamic and optical properties of selected aqueous organic and organic–inorganic mixtures of atmospheric relevance, J. Phys. Chem. A, 116, 9954–9968, 2012.

Lienhard, D. M., Huisman, A. J., Bones, D. L., Te, Y.-F., Luo, B. P., Krieger, U. K., and Reid, J. P.: Retrieving the translational diffusion coefficient of water from experiments on single levitated aerosol droplets, Phys. Chem. Chem. Phys., 16, 16677–16683, 2014.

Liu, X. and Wang, J.: How important is organic aerosol hygroscopicity to aerosol indirect forcing?, Environ. Res. Lett., 5, 044010, doi:10.1088/1748-9326/5/4/044010, 2010.

Marcolli, C. and Krieger, U. K.: Phase changes during hygroscopicity cycles of mixed organic/inorganic model systems of tropospheric aerosols, J. Phys. Chem. A, 110, 1881–1893, 2006.

Marcolli, C., Luo, B. P., Peter, Th., and Wienhold, F. G.: Internal mixing of the organic aerosol by gas phase diffusion of semivolatile organic compounds, Atmos. Chem. Phys., 4, 2593–2599, doi:10.5194/acp-4-2593-2004, 2004.

Massoli, P., Lambe, A. T., Ahern, A. T., Williams, L. R., Ehn, M., Mikkilä, J., Canagaratna, M. R., Brune, W. H., Onasch, T. B., Jayne, J. T., Petäjä, T., Kulmala, M., Laaksonen, A., Kolb, C. E., Davidovits, P., and Worsnop, D. R.: Relationships between aerosol oxidation level and hygroscopic properties of laboratory generated secondary organic aerosol (SOA) particles, Geophys. Res. Lett., 37, L24801, doi:10.1029/2010GL045258, 2010.

Mikhailov, E., Vlasenko, S., Martin, S. T., Koop, T., and Pöschl, U.: Amorphous and crystalline aerosol particles interacting with water vapor: conceptual framework and experimental evidence for restructuring, phase transitions and kinetic limitations, Atmos. Chem. Phys., 9, 9491–9522, doi:10.5194/acp-9-9491-2009, 2009.

Mochida, M. and Kawamura, K.: Hygroscopic properties of levoglucosan and related organic compounds characteristic to biomass burning aerosol particles, J. Geophys. Res., 109, D21202, doi:10.1029/2004JD004962, 2004.

Moore, R. H. and Raymond, T. M.: HTDMA analysis of multicomponent dicarboxylic acid aerosols with comparison to UNIFAC and ZSR, J. Geophys. Res., 113, D04206, doi:10.1029/2007JD008660, 2008.

Murphy, D. M., Cziczo, D. J., Froyd, K. D., Hudson, P. K., Matthew, B. M., Middlebrook, A. M., Peltier, R. E., Sullivan, A., Thomson, D. S., and Weber, R. J.: Single-particle mass spectrometry of tropospheric aerosol particles, J. Geophys. Res., 111, D23S32, doi:10.1029/2006JD007340, 2006.

Petters, M. D. and Kreidenweis, S. M.: A single parameter representation of hygroscopic growth and cloud condensation nucleus activity, Atmos. Chem. Phys., 7, 1961–1971, doi:10.5194/acp-7-1961-2007, 2007.

Pope, F. D., Harper, L., Dennis-Smither, B. J., Griffiths, P. T., Clegg, S. L., and Cox, R. A.: Laboratory and modeling study of the hygroscopic properties of two model humic acid aerosol particles, J. Aerosol Sci., 41, 457–467, 2010.

Pöschl, U.: Atmospheric aerosols: composition, transformation, climate and health effects, Angew. Chem. Int. Edit., 44, 7520–7540, doi:10.1002/anie.200501122, 2005.

Prenni, A. J., DeMott, P. J., Kreidenweis, S. M., Sherman, D. E., Russell, L. M., and Ming, Y.: The effects of low molecular weight dicarboxylic acids on cloud formation, J. Phys. Chem., 105, 11240–11248, 2001.

Prenni, A. J., DeMott, P. J., and Kreidenweis, S. M.: Water uptake of internally mixed particles containing ammonium sulfate and dicarboxylic acids, Atmos. Environ., 37, 4243–4251, 2003.

Raatikainen, T. and Laaksonen, A.: Application of several activity coefficient models to water-organic-electrolyte aerosols of atmospheric interest, Atmos. Chem. Phys., 5, 2475–2495, doi:10.5194/acp-5-2475-2005, 2005.

Renbaum-Wolff, L., Grayson, J. W., Bateman, A. P., Kuwata, M., Sellier, M., Murray, B. J., Shilling, J. E., Martin, S. T., and Bertram, A. K.: Viscosity of α-pinene secondary organic material and implications for particle growth and reactivity, P. Natl. Acad. Sci. USA, 110, 8014–8019, 2013.

Robinson, C. B., Schill, G. P., and Tolbert, M. A.: Optical growth of highly viscous organic/sulfate particles, J. Atmos. Chem., 71, 145–156, 2014.

Saukko, E., Lambe, A. T., Massoli, P., Koop, T., Wright, J. P., Croasdale, D. R., Pedernera, D. A., Onasch, T. B., Laaksonen, A., Davidovits, P., Worsnop, D. R., and Virtanen, A.: Humidity-dependent phase state of SOA particles from biogenic and anthropogenic precursors, Atmos. Chem. Phys., 12, 7517–7529, doi:10.5194/acp-12-7517-2012, 2012.

Seinfeld, J. H. and Pankow, J. F.: Organic atmospheric particulate matter, Rev. Phys. Chem., 54, 121–140, 2003.

Seinfeld, J. H. and Pandis, S. N.: Atmospheric Chemistry and Physics, 2nd edn., John Wiley & Sons, New York, NY, 2006.

Shiraiwa, M., Ammann, M., Koop, T., and Pöschl, U.: Gas uptake and chemical aging of organic aerosol particles, P. Natl. Acad. Sci. USA, 108, 11003–11008, 2011.

Shiraiwa, M., Zuend, A., Bertram, A. K., and Seinfeld, J. H.: Gas-particle partitioning of atmospheric aerosols: interplay of physical state, non-ideal mixing and morphology, Phys. Chem. Chem. Phys., 15, 1141–1453, 2013.

Sjogren, S., Gysel, M., Weingartner, E., Baltensperger, U., Cubison, M. J., Coe, H., Zardini, A. A., Marcolli, C., Krieger, U. K., and Peter, T.: Hygroscopic growth and water uptake kinetics of two-phase aerosol particles consisting of ammonium sulfate, adipic and humic acid mixtures, J. Aerosol Sci., 38, 157–171, 2007.

Song, M., Marcolli, C., Krieger, U. K., Zuend, A., and Peter, T.: Liquid–liquid phase separation and morphology of internally mixed dicarboxylic acids/ammonium sulfate/water particles, Atmos. Chem. Phys., 12, 2691–2712, doi:10.5194/acp-12-2691-2012, 2012a.

Song, M., Marcolli, C., Krieger, U. K., Zuend, A., and Peter, T.: Liquid–liquid phase separation: dependence on O : C, organic functionalities, and compositional complexity, Geophys. Res. Lett., 39, L19801, doi:10.1029/2012GL052807, 2012b.

Song, M., Marcolli, C., Krieger, U. K., Lienhard, D. M., and Peter, T.: Morphologies of mixed organic/inorganic/aqueous aerosol droplets, Faraday Discuss., 165, 289–316, 2014.

Sorooshian, A., Hersey, S., Brechtel, F. J., Corless, A., Flagan, R. C., and Seinfeld, J. H.: Rapid, size-resolved aerosol hygroscopic growth measurements: Differential Aerosol Sizing and Hygroscopicity Spectrometer Probe (DASH-SP), Aerosol Sci. Tech., 42, 445–464, 2008.

Svenningsson, B., Rissler, J., Swietlicki, E., Mircea, M., Bilde, M., Facchini, M. C., Decesari, S., Fuzzi, S., Zhou, J., Mønster, J., and Rosenørn, T.: Hygroscopic growth and critical supersaturations for mixed aerosol particles of inorganic and organic compounds of atmospheric relevance, Atmos. Chem. Phys., 6, 1937–1952, doi:10.5194/acp-6-1937-2006, 2006.

Tang, I. N.: Deliquescence properties and particle size change of hygroscopic aerosols, in: Generation of Aerosols and Facilities for Exposure Experiments, edited by: Willekie, K., Ann Arbor Science Publishers, Ann Arbor, MI, 153–167, 1980.

Tong, H.-J., Reid, J. P., Bones, D. L., Luo, B. P., and Krieger, U. K.: Measurements of the timescales for the mass transfer of water in glassy aerosol at low relative humidity and ambient temperature, Atmos. Chem. Phys., 11, 4739–4754, doi:10.5194/acp-11-4739-2011, 2011.

Vaden, T. D., Imre, D., Beranek, J., Shrivastava, M., and Zelenyuk, A.: Evaporation kinetics and phase of laboratory and ambient secondary organic aerosol, P. Natl. Acad. Sci. USA, 108, 2190–2195, 2011.

Veghte, D. P., Altaf, M. B., and Freedman, M. A.: Size dependence of the structure of organic aerosol, J. Am. Chem. Soc., 135, 16046–16049, 2013.

Virtanen, A., Joutsensaari, J., Koop, T., Kannosto, J., Yli-Pirila, P., Leskinin, J., Makela, J. M., Holopainen, J. K., Poschl, U., Kulmala, M., Worsnop, D. R., and Laaksonen, A.: An amorphous solid state of biogenic secondary organic particles, Nature, 467, 824–827, 2010.

Wise, M. W., Surratt, J. D., Curtis, D. B., Shilling, J. E., and Tolbert, M. A.: Hygroscopic growth of ammonium sulfate/dicarboxylic acids, J. Geophys. Res., 108, 4638, doi:10.1029/2003JD003775, 2003.

Xu, W., Guo, S., Gomez-Hernandez, M., Zambora, M. L., Secrest, J., Marrero-Ortiz, W., Zhang, A. L., Collins, D. R., and Zhang, R.: Cloud forming potential of oligomers relevant to secondary organic aerosols, Geophys. Res. Lett., 41, 6538–6545, 2014.

You, Y., Renbaum-Wolff, L., and Bertram, A. K.: Liquid–liquid phase separation in particles containing organics mixed with ammonium sulfate, ammonium bisulfate, ammonium nitrate or sodium chloride, Atmos. Chem. Phys., 13, 11723–11734, doi:10.5194/acp-13-11723-2013, 2013.

You, Y., Smith, M. L., Song, M., Martin, S. T., and Bertram, A. K.: Liquid–liquid phase separation in atmospherically relevant particles consisting of organic species and inorganic salts, Int. Rev. Phys. Chem., 33, 43–77, 2014.

Yu, F., Luo, G., and Ma, X.: Regional and global modeling of aerosol optical properties with a size, composition, and mixing state resolved particle microphysics model, Atmos. Chem. Phys., 12, 5719–5736, doi:10.5194/acp-12-5719-2012, 2012.

Zardini, A. A., Sjogren, S., Marcolli, C., Krieger, U. K., Gysel, M., Weingartner, E., Baltensperger, U., and Peter, T.: A combined particle trap/HTDMA hygroscopicity study of mixed inorganic/organic aerosol particles, Atmos. Chem. Phys., 8, 5589–5601, doi:10.5194/acp-8-5589-2008, 2008.

Zaveri, R. A., Easter, R. C., Fast, J. D., and Peters, L. K.: Model for Simulating Aerosol Interactions and Chemistry (MOSAIC), J. Geophys. Res., 113, D13204, doi:10.1029/2007JD008782, 2008.

Zaveri, R. A., Easter, R. C., Shilling, J. E., and Seinfeld, J. H.: Modeling kinetic partitioning of secondary organic aerosol and size distribution dynamics: representing effects of volatility, phase state, and particle-phase reaction, Atmos. Chem. Phys., 14, 5153–5181, doi:10.5194/acp-14-5153-2014, 2014.

Zhang, Q., Canagaratna, M. R., Jayne, J. T., Worsnop, D. R., and Jimenez, J. L.: Time- and size-resolved chemical composition of submicron particles in Pittsburgh: implications for aerosol sources and processes, J. Geophys. Res., 110, D07S09, doi:10.1029/2004JD004649, 2005.

Zobrist, B., Marcolli, C., Pedernera, D. A., and Koop, T.: Do atmospheric aerosols form glasses?, Atmos. Chem. Phys., 8, 5221–5244, doi:10.5194/acp-8-5221-2008, 2008.

Zobrist, B., Soonsin, V., Luo, B. P., Krieger, U. K., Marcolli, C., Peter, T., and Koop, T.: Ultra-slow water diffusion in aqueous sucrose glasses, Phys. Chem. Chem. Phys., 13, 3514–3526, 2011.

Zuend, A. and Seinfeld, J. H.: Modeling the gas-particle partitioning of secondary organic aerosol: the importance of liquid-liquid phase separation, Atmos. Chem. Phys., 12, 3857–3882, doi:10.5194/acp-12-3857-2012, 2012.

Zuend, A. and Seinfeld, J. H.: A practical method for the calculation of liquid–liquid equilibria in multicomponent organic–water–electrolyte systems using physiochemical constraints, Fluid Phase Equilibr., 337, 201–213, 2013.

Zuend, A., Marcolli, C., Luo, B. P., and Peter, T.: A thermodynamic model of mixed organic–inorganic aerosols to predict activity coefficients, Atmos. Chem. Phys., 8, 4559–4593, doi:10.5194/acp-8-4559-2008, 2008.

Zuend, A., Marcolli, C., Peter, T., and Seinfeld, J. H.: Computation of liquid-liquid equilibria and phase stabilities: implications for RH-dependent gas/particle partitioning of organic–inorganic aerosols, Atmos. Chem. Phys., 10, 7795–7820, doi:10.5194/acp-10-7795-2010, 2010.

Zuend, A., Marcolli, C., Booth, A. M., Lienhard, D. M., Soonsin, V., Krieger, U. K., Topping, D. O., McFiggans, G., Peter, T., and Seinfeld, J. H.: New and extended parameterization of the thermodynamic model AIOMFAC: calculation of activity coefficients for organic-inorganic mixtures containing carboxyl, hydroxyl, carbonyl, ether, ester, alkenyl, alkyl, and aromatic functional groups, Atmos. Chem. Phys., 11, 9155–9206, doi:10.5194/acp-11-9155-2011, 2011.

Table 1. Aerosol systems studied.

Aerosol System	Organic-Component Structures	Organic : Inorganic Dry Mass Ratio	Previous Experimentally-Determined Phase Behavior	References
Citric Acid + Ammonium Sulfate	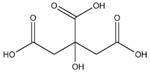	2 : 1	No LLPS observed	You et al. (2012)
Diethylmalonic Acid + Ammonium Sulfate	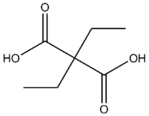	2 : 1	LLPS at RH ≤ 89 %	You et al. (2012)
2-Methylglutaric Acid + Ammonium Sulfate	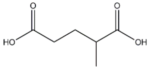	2 : 1	LLPS at RH ≤ 75 %	You et al. (2012)
C_5 dicarboxylic acids mixture (glutaric, methylsuccinic, dimethly-malonic) + Ammonium Sulfate	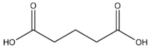 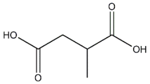 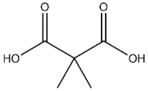	1 : 1	No LLPS observed	Song et al. (2012a)
C_6 dicarboxylic acid mixture (2-methylglutaric, 3-methylglutaric, 2,2-dimethylsuccinic) + Ammonium Sulfate	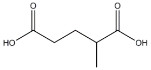 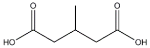 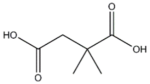	1 : 1	Transition from LLPS with partially-engulfed morphology to single liquid phase at RH = 74 %	Song et al. (2012a)

Table 1. Continued.

Aerosol System	Organic-Component Structures	Organic : Inorganic Dry Mass Ratio	Previous Experimentally-Determined Phase Behavior	References
C_7 dicarboxylic acid mixture (3-methyladipic, 3,3-dimethylglutaric, diethylmalonic) + Ammonium Sulfate	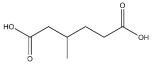 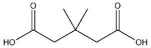 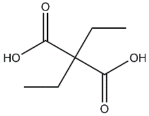	1 : 1	Transition from LLPS with core-shell morphology to single liquid phase at RH = 89–90 %	Song et al. (2012a)
Sucrose	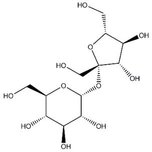	N/A	Glass transition at RH = 24–53 %, depending on timescale of RH change	Tong et al. (2011), Zobrist et al. (2011)
Sucrose + Ammonium Sulfate		1 : 1	Unknown	This study
Sucrose + Ammonium Sulfate		2 : 1	Unknown	This study

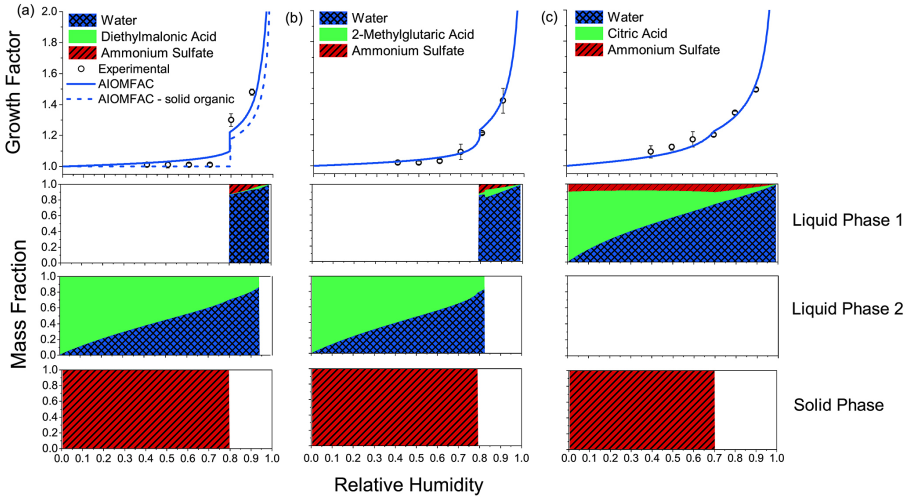

Figure 1. Top panels: measured and AIOMFAC-predicted hygroscopic diameter growth factors for **(a)** diethylmalonic acid–ammonium sulfate particles, **(b)** 2-methylglutaric acid–ammonium sulfate particles, and **(c)** citric acid–ammonium sulfate particles, with dry organic : inorganic mass ratios of 2 : 1 for all systems. The black circles indicate the average growth factor measured across ten experiments and error bars indicate the SD of the measured growth factors. Panels below the hygroscopic growth curves indicate the AIOMFAC-predicted composition of each of three possible phases present in the particles (liquid phase 1, liquid phase 2, and a solid phase) as a function of relative humidity. Empty boxes indicate that no second liquid phase is predicted.

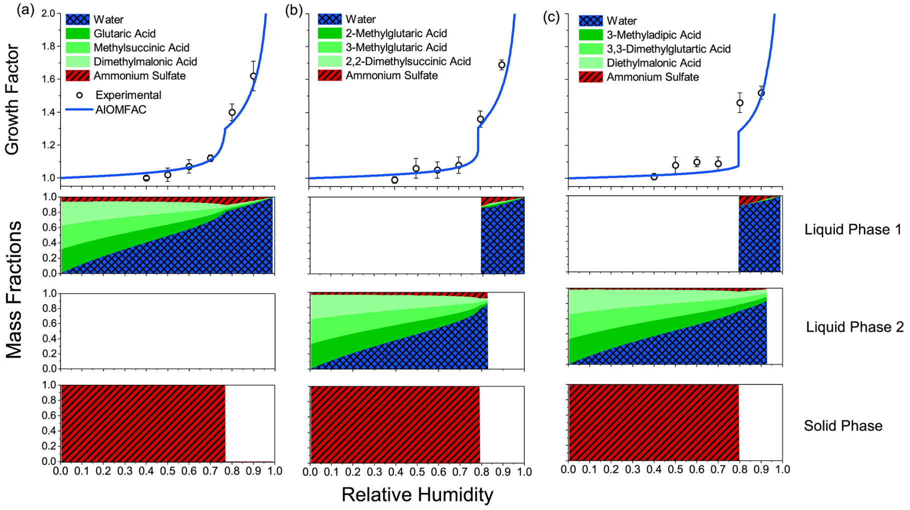

Figure 2. Top panels: measured and AIOMFAC-predicted hygroscopic diameter growth factors for **(a)** C_5 dicarboxylic acid mixture–ammonium sulfate particles, **(b)** C_6 dicarboxylic acid mixture–ammonium sulfate particles, and **(c)** C_7 dicarboxylic acid mixture–ammonium sulfate particles, with dry organic : inorganic mass ratios of 1 : 1 for all systems. The black circles indicate the average growth factor measured across ten experiments and error bars indicate the SD of the measured growth factors. Panels below the hygroscopic growth curves indicate the AIOMFAC-predicted composition of each of three possible phases present in the particles (liquid phase 1, liquid phase 2, and a solid phase) as a function of relative humidity. Empty boxes indicate that no second liquid phase is predicted.

Title Page
Abstract
Introduction
Conclusions
References
Tables
Figures
◀◀
▶▶
◀
▶
Back
Close
Full Screen / Esc
Printer-friendly Version
Interactive Discussion

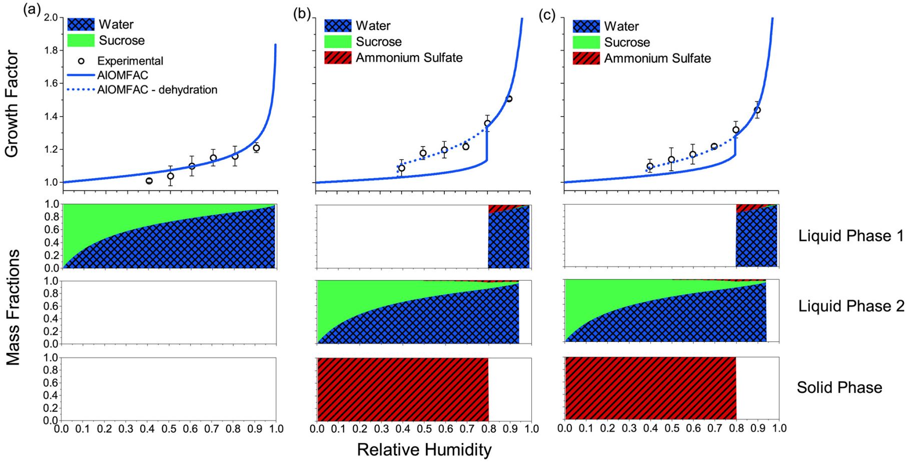

Figure 3. Top panels: measured and AIOMFAC-predicted hygroscopic growth factors for **(a)** sucrose particles, **(b)** mixed sucrose–ammonium sulfate particles with an organic : inorganic ratio of 1 : 1, and **(c)** mixed sucrose–ammonium sulfate particles with an organic : inorganic ratio of 2 : 1. The black circles indicate the average growth factor measured across ten experiments and error bars indicate the SD of the measured growth factors. Solid lines indicate the hydration curve calculated with the AIOMFAC-based equilibrium model, while dashed lines illustrate the dehydration branch in which a supersaturated solution is present with respect to the dissolved ammonium sulfate. The three panels below the hygroscopic growth curves indicate the AIOMFAC-predicted composition of each of three possible phases present in the particles during the hydration process (liquid phase 1, liquid phase 2, and a solid phase) as a function of relative humidity. Empty boxes indicate that no second liquid phase or no solid phase is predicted.

Title Page
Abstract | Introduction
Conclusions | References
Tables | Figures
◀▮ | ▮▶
◀ | ▶
Back | Close
Full Screen / Esc
Printer-friendly Version
Interactive Discussion

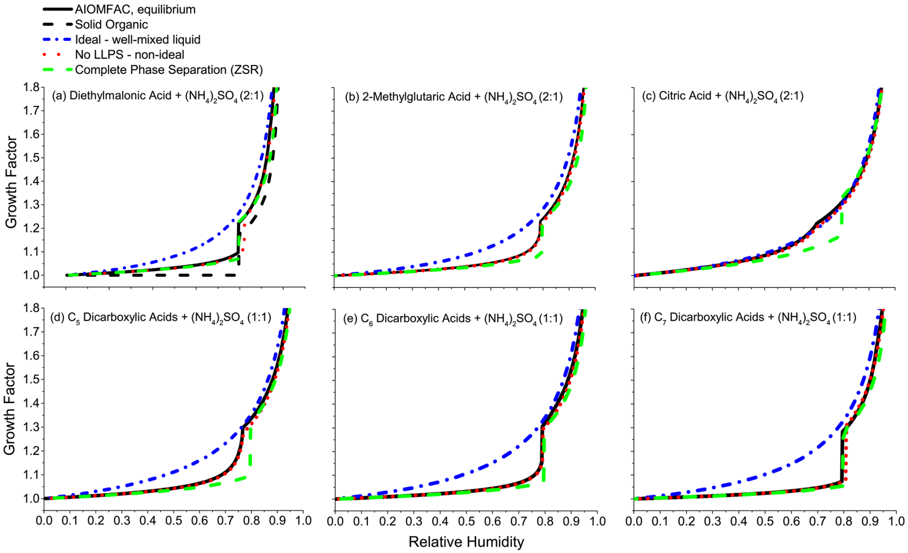

Figure 4. Comparison of simplified thermodynamic assumptions to the full AIOMFAC hygroscopic growth calculations for the multi-component systems for which we expect that observed water-uptake behavior is governed by thermodynamic equilibrium conditions. Organic : inorganic dry mass ratios, which can substantially influence the extent to which non-ideal interactions affect water-uptake, are given in parentheses. The performance of the simplified modeling approaches varies across the systems with variations in phase behavior. Disagreement between the full AIOMFAC-based equilibrium calculations and the simplified models is greatest at low to moderate RH (RH = 20–80 %).

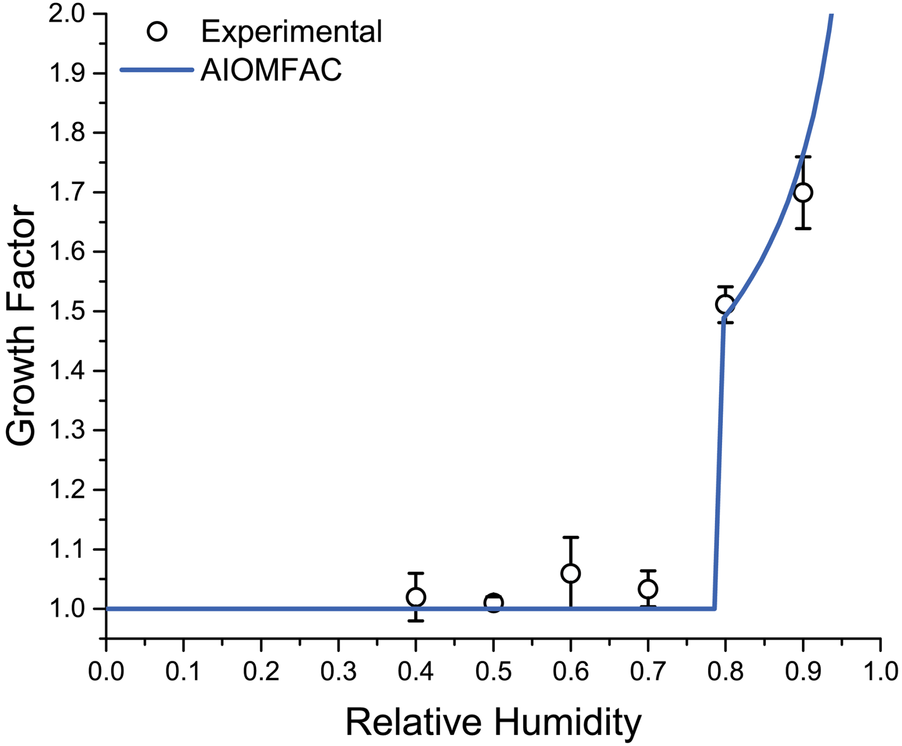

Figure B1. Measured and modeled hygroscopic growth factors for ammonium sulfate particles with dry mobility diameters of 250 nm. The black circles indicate the average growth factor measured across ten experiments and error bars indicate the SD of the measured growth factors.